Journal of Physics: Conference Series **303** (2011) 012007 doi:10.1088/1742-6596/303/1/012007

Employing magnonic crystals to dictate the characteristics of auto-oscillatory spin-wave systems

A D Karenowska[1], A V Chumak[2], A A Serga[2], J F Gregg[1] and B Hillebrands[2]

[1] Department of Physics, Clarendon Laboratory, University of Oxford, OX1 3PU Oxford, United Kingdom

[2] Fachbereich Physik and Forschungszentrum OPTIMAS, Technische Universität Kaiserslautern, 67663 Kaiserslautern, Germany

E-mail: a.karenowska@physics.ox.ac.uk

Abstract. Spin-wave active rings—positive-feedback systems incorporating spin-wave waveguides—provide important insight into fundamental magnetics, enable experimental investigations into nonlinear wave phenomena, and potentially find application in microwave electronics. Such rings break into spontaneous, monomode oscillation at a certain threshold value of feedback gain. In general, the wavenumber of this initially excited, threshold mode is impossible to predict precisely. Here we discuss how, by exploiting resonant spin-wave reflections from a magnonic crystal, an active ring system having a threshold mode with a well-defined and precisely predictable wavenumber may be realized. Our work suggests that study and development of active ring systems incorporating magnonic crystals may deliver useful insight into spin-wave transmission in structured magnetic films as well as devices with technological applicability.

1. Introduction

Magnetostatic spin waves (MSWs) typically have microwave (GHz) frequencies and wavelengths in the micron to millimetre range [1]. The study of MSW spectra has long been recognized for the important insight it provides into the underlying physics of static and dynamic magnetism. Moreover, because of the short wavelengths, low velocities, and rich dispersion characteristics of these excitations, MSW systems provide useful model environments for the study of general wave and quasi-particle phenomena (see for example [2–6] and references therein) and are widely acknowledged for their potential to provide a platform for spintronic information transfer and transport (see for example [7, 8]).

One material in particular, the ferrimagnet yttrium iron garnet $Y_3Fe_5O_{12}$ (YIG), dominates experimental studies into MSW dynamics. At around 0.04 kAm^{-1} (0.5 Oe) the ferrimagnetic resonance (FMR) linewidth of monocrystalline YIG is the narrowest of any known material. Magnon lifetimes of order hundreds of nanoseconds allow spin-wave propagation to be observed over centimetre distances, and large higher order terms in the garnet's dynamic magnetic susceptibility permit nonlinear propagation phenomena to be observed and studied at extremely low signal powers [6].

MSW propagation in YIG-based auto-exciting spin-wave oscillators or "active rings" has for some time been an area of interest within the field. Such systems comprise a thin-film YIG

waveguide with spin-wave excitation and reception antennas connected together via a variable gain electrical positive-feedback path. If the feedback gain is sufficiently high, the ring supports noise-initiated, self-sustained propagating oscillations. As well as enabling investigations into the intrinsic dynamic properties of magnetic systems, YIG-based active rings also facilitate the experimental study of a range of exotic linear and nonlinear wave behaviours, for example soliton [3, 5, 9] and bullet [10] generation, fractal formation [11], and chaotic processes [12, 13], applicable to but not readily observable in other physical domains.

The majority of experimental studies of MSW dynamics in YIG are undertaken in thin-film waveguides under conditions of external, unidirectional magnetic bias. MSW propagation in such systems is strongly anisotropic and several distinct categories of waves, having markedly different characteristics, are identified [1, 6]. The waves are classified according to the relative orientation of the their propagation direction and the bias field. Backward volume magnetostatic spin waves (BVMSW), associated with an in-plane magnetic bias parallel to the spin-wave propagation direction, have latterly attracted particular interest in the context of active ring studies because of their unusual dispersion properties; the gradient of the BVMSW dispersion curve $\omega(k)$ is negative and thus the waves' group and phase velocities have opposite directions and short wavelengths are associated with low frequencies.

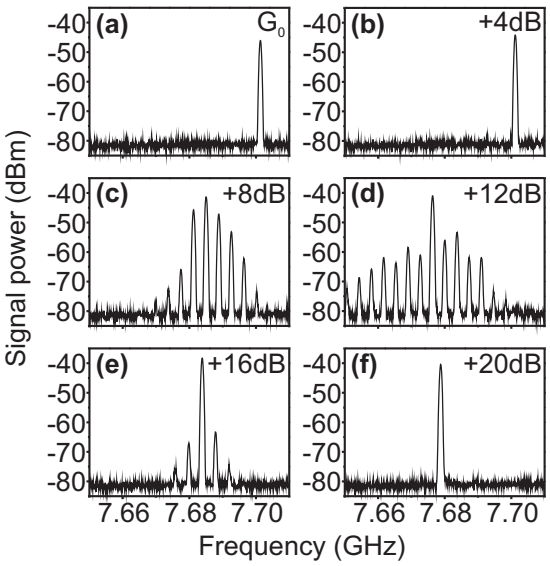

Figure 1. Excitation spectra of a simple BVMSW active ring as the feedback gain is varied from a starting value G_0 (a) to a value 20 dB above this (f). Excitation initiates at a threshold value of feedback gain. The frequency of the threshold mode lies in the lowest loss region of the spin-wave passband of the waveguide included in the loop but its precise wavenumber is almost impossible to predict. Monomode excitation persists ((a) and (b)) until a second threshold beyond which nonlinear splitting processes permit excitations at multiple k-values. The subsequent evolution of the spectrum is extremely complex and includes multi- and monomode regimes ((c) to (f)).

Excitation of a simple YIG-based BVMSW active ring initiates at a threshold value of feedback gain; the self-generation threshold. At this threshold, the ring signal is monochromatic, its wavenumber $k = k_t$ corresponds to the lowest loss phase-feasible mode, and its amplitude is regulated by the magnetic nonlinearity of the waveguide. If the gain is further increased, the presence of this threshold mode suppresses all others until a second, higher threshold beyond which nonlinear splitting processes permit the excitation of waves with multiple k-values and the system becomes multimoded. By way of example, Fig. 1 shows the excitation spectrum of such a system as the feedback gain is varied from a value G_0 in the monomode regime (a) to a value 20 dB above this level (f). The evolution of the spectral content of the ring oscillations in response to gain variations is too complex to be amenable to precise theoretical analysis, but certain signal categories can be identified and, depending on the magnetic bias conditions and the ring geometry, a range of interesting nonlinear behaviours can be observed, many of which, as alluded to above, have been subject to detailed study [3, 5, 9–13]. However, as well as these

multimode, high-gain regimes, the monomode behaviour observed when the feeedback gain is at and just beyond the self-generation threshold is also very interesting. Not only does studying the competitive process of oscillation initiation offer physical insight into the magnetic properties of the waveguide in the loop, but, since the linewidth of the threshold mode is typically very narrow (of order kHz or tens of kHz), rings operating in this signal regime potentially find application in high-Q oscillators and other microwave devices.

The mode excited at the self-generation threshold k_t is the lowest loss mode for which the net phase shift around the ring is an integer multiple of 2π (phase feasibility). From a knowledge of the transmission characteristics of the spin-wave waveguide in a given ring subject to a given magnetic bias, it is possible to make a crude estimate of the frequency—and thus wavenumber—range within which this mode will fall. However, owing to a complex dependence on a wide range of intrinsic and extrinsic experimental parameters, its *precise* wavenumber is almost impossible to predict. This is disadvantageous from an applications perspective where, in many cases, a deterministic system is desirable.

A magnonic crystal is an artificially engineered spin-wave transmission structure with spatially periodic variations in its magnetic properties. The spin-wave analogue of an optical photonic or acoustic phononic crystal; the transmission characteristics of a magnonic crystal feature band gaps: frequency bands over which, due to resonant interactions with the artificial crystal lattice, the propagation of spin waves is strongly suppressed [14–21]. By analogy with X-ray or neutron diffraction in a natural crystalline solid, the wavenumbers corresponding to the n^{th} BVMSW band gaps of a one dimensional magnonic crystal with lattice constant a are those which satisfy the Bragg condition at normal incidence:

$$k = n\frac{\pi}{a}, \qquad \text{where} \quad n = 1, 2, 3, 4, \ldots . \tag{1}$$

If spin waves with these k-values are incident on the crystal, they are strongly reflected.

In this paper, we describe how a magnonic crystal can be used to create a BVMSW active ring structure in which the wavenumber k_t of the threshold mode takes a single, well-defined value [22].

2. Methods

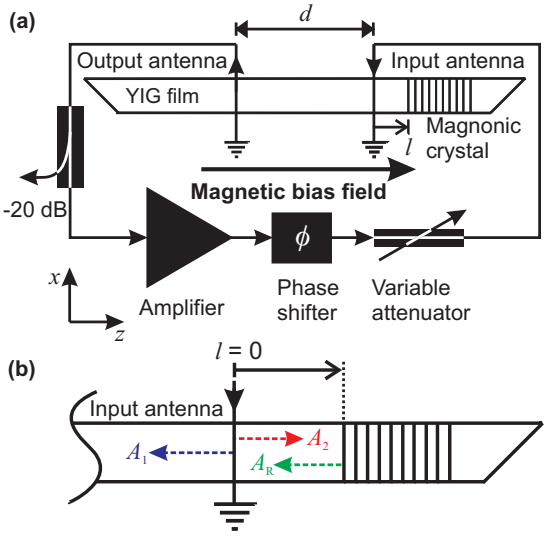

Figure 2. (a) Schematic diagram of the experimental BVMSW active ring system. Two microstrip antennae (width 50 μm), a distance $d = 8$ mm apart excite (input) and detect (output) propagating spin waves in a thin-film YIG waveguide. A magnonic crystal, etched into the surface of the film, is positioned a distance l from the input antenna. l can be varied with precision ±5 μm. A bias magnetic field of 160.4 kAm^{-1} (2016 Oe) is applied in-plane, parallel to the spin-wave propagation direction (the z-axis) (b) Expanded plan view of the region proximal to the input antenna.

The experimental active ring system is shown in Fig. 2. Microstrip spin-wave input (right) and output (left) antennae are in contact with the surface of a narrow YIG waveguide magnetically

biased parallel to its long axis. The antennae are connected via an electrical feedback network comprising a phase shifter (phase shift ϕ), an amplifier, a variable attenuator and a directional coupler. The combination of the amplifier and the attenuator control the feedback gain whilst the coupler allows the ring signal to be sampled. The majority of the YIG film is of uniform thickness (5.5 μm) but, offset from its centre, is a short one-dimensional magnonic crystal [14–21] comprising ten grooves of width 30 μm, depth 300 nm and spacing 270 μm (lattice constant $a = 300$ μm) [20]. This crystal is positioned with its first groove a distance l from the input antenna. l can be varied by translating the film relative to the fixed antennae.

Figure 3 illustrates the BVMSW transmission characteristics of the homogeneous region of the film (solid, blue) and the magnonic crystal (dotted, red). The FMR frequency is approximately 7.710 GHz. Band gaps in the magnonic crystal characteristic corresponding to the first three Bragg orders (Eq. 1) are clearly visible. The low loss region of the spin-wave passband just below the FMR frequency (Band A) and the first band gap of the magnonic crystal (Band B) are the focus of the discussion which follows.

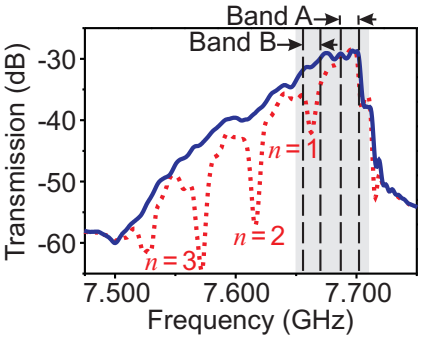

Figure 3. BVMSW transmission characteristics for the uniform (solid, blue) film and the magnonic crystal (dotted, red) used in the study. The n^{th} order band gaps of the magnonic crystal are indicated. Band A identifies the lowest loss region of the spin-wave passband of the uniform film, Band B, the first band gap of the magnonic crystal.

Upon excitation, the input antenna drives propagating spin waves both toward the output antenna (blue, complex amplitude A_1 in Fig. 2(b)) and toward the magnonic crystal (red, complex amplitude A_2). If the spin-wave wavenumber satisfies Eq. 1 the wave incident on the magnonic crystal is reflected (green, complex amplitude A_{R}) and propagates back toward the input antenna.

Left and right-going waves have a relative phase of π [23] and it is also found experimentally that an effective phase shift of π (referenced to l) is associated with reflection from the magnonic crystal. Thus, the total phase accumulation of a reflected signal (satisfying Eq. 1) between transmission from the input antenna and arrival back at this point in the waveguide is $\phi_l = 2kl$. It follows that if it can be arranged that

$$\phi_l = 2\pi n\frac{l}{a} = 2\pi m, \qquad \text{where} \quad n = 1, 2, 3, 4, \ldots \quad \text{and} \quad m = 0, 1, 2, 3, \ldots, \tag{2}$$

the reflected signal will act to enhance the effective loop gain. If this enhancement is sufficient to increase the gain of a phase-feasible mode lying within a band gap of the magnonic crystal over and above the value associated with the lowest loss region of the passband of the uniform film (Band A, Fig. 3) then there is provided a mechanism by which this mode—the wavenumber of which is rigidly fixed by the geometry of the magnonic crystal—may be preferentially excited at the self-generation threshold.

The maximum possible increase in loop gain through reflection from the magnonic crystal is 3 dB. It is clear therefore from the data of Fig. 3, that for our particular experimental system, only spin-wave modes associated with the first band gap (Band B, Fig. 3) may be promoted to dominance via this mechanism, since the transmission loss at k-values corresponding to all higher-order gaps is at least 10 dB in excess of that associated with the lowest loss region of

the passband (Band A). A theoretical model predicts an enhancement effect associated with $k = k_1 = \pi/a = 104.72$ rad/cm (Eq. 1) centred on 7.663 GHz, for the experimental ring, accessible for integer values of the ratio l/a (Eq. 2).

3. Results

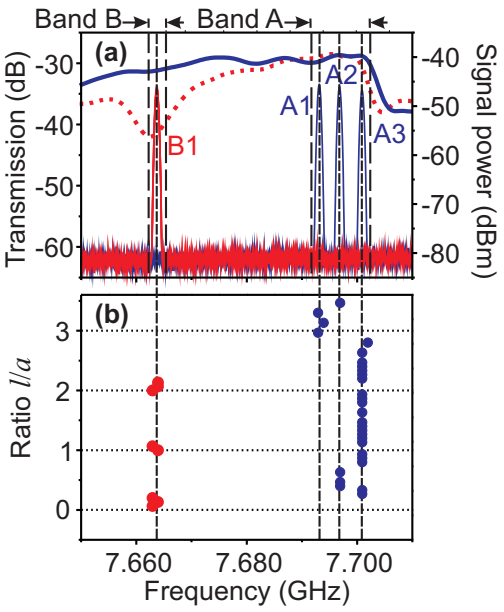

Figure 4. (a) The solid blue and dotted red curves (left ordinate axis) show the transmission characteristics of (respectively) the uniform region of the YIG film and the magnonic crystal over the frequency range 7.650–7.710 GHz (the grey shaded region of Fig. 3). The inset diagram is a composite of overlaid ring power spectra captured via the -20 dB directional coupler of Fig. 2(b). Each spectrum comprises a single peak corresponding to the threshold mode k_t. As indicated in (b), modes A1, A2 and A3 positioned within the low loss region of the spin-wave passband (Band A) correspond to general values of the ratio l/a (blue circles), whilst the mode B1 which lies within the first band gap of the magnonic crystal at $k = k_1$ (Band B) is observed at and only at integer values (red circles). Note that data has been compensated for temperature variations.

An expanded view of the transmission curves of Fig. 3 over the frequency range 7.650–7.710 GHz is shown in Fig. 4(a) (left ordinate axis). Overlaid, are experimental power spectra of threshold modes corresponding to a range of values of the ratio l/a between zero ($l = 0$) and 3 ($l = 900$ nm) (right ordinate axis). In order to collect these data, at each measured value of l, the feedback gain was increased via the variable attenuator (Fig. 2(a)) from a value below the self-generation threshold (i.e. from an inactive state of the ring) to a value 5 dB above it and the spectrum of the ring signal recorded. Each spectrum contains a single peak. (Note that the sharpness of the spectral peaks shown is limited by the scanning window of the spectrum analyzer, their true width is ≤ 25 kHz.) For general l/a, the wavenumber of the threshold mode k_t is determined solely by gain and phase feasibility conditions. As anticipated in the discussion above, the mode lies in the lowest loss region of the spin-wave passband (Band A, modes A1, A2 and A3), but a precise prediction of the value of k_t is not possible. By contrast, for integer l/a, the wavenumber selective magnonic crystal reflection mechanism enhances the effective ring gain of the mode $k = k_1$ associated with the first band gap of the magnonic crystal, forcing $k_t = k_1$. Figure 4(b) shows the l/a dependence of k_t for a fixed input phase ϕ at the phase shifter (tuned for feasibility of the k_1 mode). Each point corresponds to a separate experiment performed using an identical technique to that described in connection with the spectra of Fig. 4(a). The maximum integer value of l/a at which k_1 mode promotion is observed is 2. Beyond this value, the loss associated with the signal path of the reflected wave reduces the loop gain at k_1 below that for the lowest loss mode associated with the uniform region of the film.

In an ideal system, with fixed external phase shift ϕ we would expect to observe one of just two threshold modes at a given l: one in the low loss region of the spin-wave passband (Band A, Fig. 4(a)) associated with general k and l/a and a second at and only at integer l/a

with wavenumber k_1 (Band A). The fact that three separate modes are observed in Band A is an artifact of the experimental method; it is due to the fact that the thickness and thus the dispersion relationship $\omega(k)$ of the YIG film is not perfectly uniform along its length, providing a secondary mechanism for the phase accumulation around the ring to vary as a function of l independently of ϕ [22].

4. Conclusions

In summary, it has been demonstrated that the wavenumber selective reflectivity of a magnonic crystal can be exploited to create a BVMSW active ring system which will commence monomode auto-oscillation at precise wavenumber. This wavenumber corresponds the first band gap of the crystal and, as such, is readily determinable from its lattice constant. Such high-Q, wavenumber selective active ring arrangements may find practical application in microwave oscillators, spin-wave logic systems and sensor instrumentation. Moreover, this work suggests that by further pursuing their development and investigation we may obtain useful insight into the complex mechanism of spin-wave reflection from magnonic crystal structures.

Acknowledgments

Financial assistance from the DFG (grant numbers SE 1771/1-1 and GRK 792), and technical support from the Nano+Bio Centre, TU Kaiserslautern are gratefully acknowledged. ADK acknowledges the support of the IET Leslie H. Paddle Scholarship and Magdalen College, Oxford.

References

[1] Stancil D D 1993 *Theory of Magnetostatic Waves* (New York: Springer-Verlag)
[2] Schneider T, Serga A A, Chumak A V, Sandweg C W, Trudel S, Wolff S, Kostylev M P, Tiberkevich V S, Slavin A N and Hillebrands B 2010 *Phys. Rev. Lett.* **104** 197203
[3] Wu M and Patton C E 2007 *Phys. Rev. Lett.* **98** 047202
[4] Demokritov S O, Demidov V E, Dzyapko, O, Melkov, G A, Serga, A A, Hillebrands, B and Slavin A N 2006 *Nature* **443** 430
[5] Demokritov S O, Serga A A, Demidov V E, Hillebrands B, Kostylev M P and Kalinikos B A 2003 *Nature* **426**, 159
[6] Serga A A, Chumak A V and Hillebrands B 2010 *J. Phys. D* **43** 264002
[7] Kajiwara Y, Harii K, Takahashi S, Ohe J, Uchida K, Mizuguchi M, Umezawa H, Kawai H, Ando K, Takanashi K, Maekawa S and Saitoh E 2010 *Nature* **464** 262
[8] Schneider T, Serga A A, Leven B, Hillebrands B, Stamps R L and Kostylev M P 2008 *Appl. Phys. Lett.* **92** 022505
[9] Kalinikos B A, Kovshikov N G, and Patton C E 1998 *Phys. Rev. Lett.* **80** 4301
[10] Serga A A, Demokritov S O, Hillebrands B and Slavin A N 2004 *Phys. Rev. Lett.* **92** 117203
[11] Wu M, Kalinikos B A, Carr L D, and Patton C E 2006 *Phys. Rev. Lett.* **96**, 187202
[12] Wu M, Hagerstrom A M, Kondrashov A and Kalinikos B 2009 *Phys. Rev. Lett.* **102** 237203
[13] Hagerstrom A M, Tong W, Wu M, Kalinikos B A and Eykholt R 2009 *Phys. Rev. Lett.* **102** 207202
[14] Chumak A V, Serga A A, Wollf S, Hillebrands B and Kostylev M P 2009 *Appl. Phys. Lett.* **94** 172511
[15] Chumak A V, Serga A A, Wollf S, Hillebrands B and Kostylev M P 2009 *J. Appl. Phys.* **105** 083906
[16] Lee K S, Han D S and Kim S K 2009 *Phys. Rev. Lett.* **102** 127202
[17] Ustinov A B, Kalinikos B A, Demidov V E and Demokritov S O 2009 *Phys. Rev. B* **80** 052405
[18] Wu M, Hagerstrom A M, Eykholt R, Kondrashov A and Kalinikos B A 2009 *Phys. Rev. Lett.* **102** 237203
[19] Wang Z K, Zhang V L, Lim H S, Ng S C, Kuok M H, Jain S and Adeyeye A O 2009 *Appl. Phys. Lett.* **94** 083112
[20] Chumak A V, Serga A A, Hillebrands B and Kostylev M P 2008 *Appl. Phys. Lett.* **93** 022508
[21] Sykes C G, Adam J D and Collins J H 1976 *Appl. Phys. Lett.* **29** 388
[22] Karenowska A D, Chumak A C, Serga A A, Gregg J F and Hillebrands B 2010 *Appl. Phys. Lett.* **96** 082505
[23] Schneider T, Serga A A, Neumann T, Hillebrands B and Kostylev M P 2008 *Phys. Rev. B* **77** 214411